Surface-Modified Gold Nanoparticles Possessing Two-Channel Responsive Eu(III)/Tb(III) Cyclen Complexes as Luminescent Logic Gate Mimics

Laura K. Truman, Samuel J. Bradberry,* Steve Comby, Oxana Kotova, and Thorfinnur Gunnlaugsson*[a]

The development of material-supported molecular logic gate mimics (MGLMs) for contained application and device fabrication has become of increasing interest. Herein, we present the formation of ≈5 nm gold nanoparticles (AuNPs) that have been surface-modified (via a thiol linkage) with heptadentate cyclen-based complexes of europium and terbium for sensing applications using delayed lanthanide luminescence and as integrated logic gate mimics within competitive media.

The development of responsive luminescent molecules and materials is an active area of research within supramolecular chemistry.[1] Molecules that can respond logically to external stimuli, or "inputs", that affect/modulate their photophysical properties, or "outputs", have been known since the pioneering independent work of de Silva and Aviram.[2] Where the modulation in the output is dependent upon more than one "input", molecular logic gate mimics (MLGMs) of increasing complexity can arise. Such inputs can be in the form of ions and molecules, while the output can be regarded, as stated above, as a change in various photophysical properties (such as intensity, excited state lifetime, wavelength, etc.). In the case of simple organic, or coordination compounds,[3] potential "outputs" can be a characteristic change in both the absorption or the emission spectra of a compound.[4] These have been demonstrated elegantly by de Silva,[5] Andreasson,[6] and Pischel[7] amongst others.[8] Through our own work, we have demonstrated that lanthanide (Ln(III)) complexes can be used in solution as single MLGMs,[9] sensors[10] and in parallel processes,[11] exploiting their characteristic emission properties.[12] Logical analysis provides a universal language to describe responsive changes from simple "on-off" sensors to more complex multi-stimuli systems.[13] Although, solution-based MLGMs have a well-established history, there has only been a recent attention on their application on, and within, materials platforms. Recently, we demonstrated that MLGMs can be incorporated

into soft material like polymeric gels and employed this in delivery of cargo.[14] Medintz and co-workers showed metal-supported MLGMs, modifying the surface of CdSe/Zns QDs with Tb(III) complexes and an organic dye allowing the use of FRET processes, including participation of the QD itself, to generate a versatile array of MLGMs including AND, OR, INH, NAND and XOR logic functions.[15] A similar and common inorganic support that has been utilized in both sensing and imaging, are AuNP structures, which are functionalized at the metal surface by attachment through thiol groups.[16] We have demonstrated the use of AuNPs functionalised with emissive Ln(III) complexes for the formation of selective luminescence probes,[17] imaging agents,[18] and AuNP-based displacement assays for organic molecules.[19] In this Communication, we combine our interest in material and sensing chemistry, by presenting an example of surface modification of AuNPs with luminescent ternary complexes that are responsive, resulting in modulation of luminescent "outputs" that can be expressed in terms of molecular logic functions. Our design is based on two cyclen (1,4,7,10-tetraazacyclododecane) Ln(III) complexes, using Eu(III) and Tb(III), both formed from the same common ligand **1**, which was tethered to the surface of 5 nm gold nanoparticles using thiol chemistry (Figure 1). The AuNP-immobilised complexes are responsive to H+ and showed Ln(III)-centred luminescent responses. However, as coordinatively unsaturated complexes, the emission response is weak due to quenching by O-H oscillators from solvent water. The formation of ternary complexes with appropriate aromatic ligands, termed the "antennae", could be achieved, which displaces the lanthanide bound water molecules, resulting in coordinatively saturated complexes which in comparison are highly emissive.[20] The appropriate selection of ter-
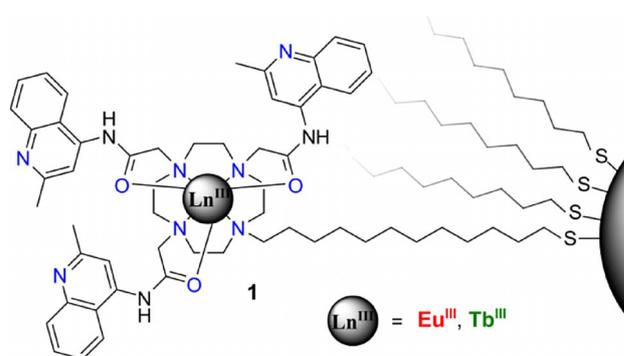
[a] Dr. L. K. Truman, S. J. Bradberry, Dr. S. Comby, Dr. O. Kotova,
Prof. Dr. T. Gunnlaugsson
School of Chemistry and Trinity Biomedical Sciences Institute
Trinity College Dublin
152–160 Pearse Street, Dublin, Dublin 2 (Ireland)
E-mail: bradbers@tcd.ie
gunnlaut@tcd.ie

Supporting Information and the ORCID identification number(s) for the
author(s) of this article can be found under:
https://doi.org/10.1002/cphc.201700440.

An invited contribution to a Special Issue on Molecular Logic

Figure 1. Structure of AuNPs functionalised with **[Ln.(1)]³⁺** complexes (Ln = Eu(III) or Tb(III)) through thiol linkages.

nary ligands that preferentially sensitise Eu[III] or Tb[III] ions as "input species", that is, (4,4,4-trifluoro-1-(naphthalene-2-yl)-butane-1,3-dione (nta) and 4-(dimethylamino)benzoic acid (DMAB), respectively) allowed for independent responses in the two Ln[III] emissions to be achieved. These responses, as double-displacement-assay systems, were then analysed in terms of molecular logic, allowing for parallel processing to be achieved.

The synthesis of ligand **1** was achieved through the mono-substitution of the cyclen macrocycle with dodecanethiol followed by the sequential (triple) substitution with 2-chloro-N-2-methyl-quinolin-4-yl-acetamide,[21] which also functions as a sensitising antenna for the Eu[III] and Tb[III] emission. Complexes were formed from **1** with Eu(CF$_3$SO$_3$)$_3$ and Tb(CF$_3$SO$_3$)$_3$ in CH$_3$OH under microwave irradiation in 90% yields. The synthesis and characterisation of **1**, **[Eu.1]$^{3+}$** and **[Tb.1]$^{3+}$** can be found in the Supporting Information. The luminescence lifetime measurements of **[Eu.1]$^{3+}$** and **[Tb.1]$^{3+}$** recorded in H$_2$O and D$_2$O indicated a single water molecule bound to the Ln[III] centres ($q_{Eu,Tb} \approx 1$). This water molecule was displaced by the nta or DMAB antennae, resulting in modulation of the emission and change in from 1 to $q_{Eu,Tb} \approx 0$. For such complexes, a q-value of 2 would be expected, but our previous work in the area has demonstrated that the thiol moiety can also bind to the metal ion centre, resulting in a lover q-value.[22a] This was confirmed by synthesising an analogue of **1**, which lacked the thiol functionality, resulting in a q-value of 2.

AuNPs were synthesised through using a modified Brust–Schiffrin method[23] and coated with **[Eu.1]$^{3+}$**, **[Tb.1]$^{3+}$** or a 1:1 ratio by treating the synthesized AuNPs with appropriate solutions of **[Eu.1]$^{3+}$** or **[Tb.1]$^{3+}$** in 99% H$_2$O:DMSO.[22a] The resulting functionalised AuNPs were characterised by transmission electron microscopy (TEM) and dynamic light scattering (DLS), demonstrating the formation of spherical AuNPs (PDI 0.42, by DLS) with an average hydrodynamic diameter of ca. 14 ± 2 nm (Figure 2). UV-visible absorption measurements also confirmed the successful surface functionalization with a red shift in the surface plasmon resonance (SPR) band. No changes were seen in the absorption band over periods of many months demonstrating that **AuNP-[Eu.1]$^{3+}$**, **AuNP-[Tb.1]$^{3+}$** and **AuNP-[Eu.1]$^{3+}$/[Tb.1]$^{3+}$** were stable in aqueous solution at RT. The discussion herein will mainly focus on the AuNP systems (see the Supporting Information for details on **[Eu.1]$^{3+}$** and **[Tb.1]$^{3+}$**)
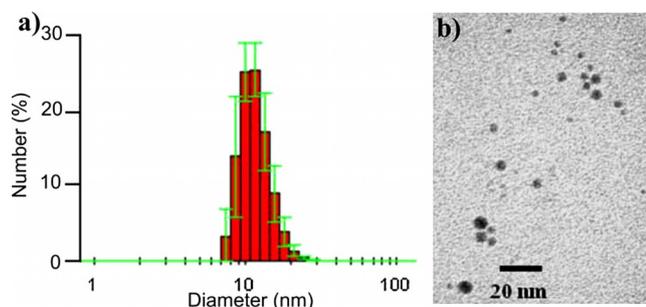

Figure 2. a) Size distribution of **AuNP-[Eu.1]$^{3+}$/[Tb.1]$^{3+}$** in aqueous solution as measured by DLS; b) TEM image of **AuNP-[Eu.1]$^{3+}$/[Tb.1]$^{3+}$** deposited from an aqueous solution. Scale bar in (b) = 20 nm.

The photophysical properties of **[Eu.1]$^{3+}$** and **[Tb.1]$^{3+}$** as well as **AuNP-[Eu.1]$^{3+}$** and **AuNP-[Tb.1]$^{3+}$** were probed using absorption and luminescence spectroscopy. The UV-visible absorption spectrum of **AuNP-[Eu.1]$^{3+}$** from 250–800 nm and the corresponding spectrum from **AuNP-[Tb.1]$^{3+}$** can be found in the Supporting Information. A structure consistent with complexes **[Eu.1]$^{3+}$** and **[Tb.1]$^{3+}$** in solution was observed, the absorption maximum at 318 nm (log = 4.4) was appropriate for excitation and sensitisation of Ln[III]-centred emission (this also being confirmed by monitoring the excitation spectra of the complexes). A broad absorption ($\lambda_{max} = 540$ nm) was also observed, corresponding to the SPR of the AuNPs, which was red-shifted ca. 6 nm compared to the non-functionalised AuNPs; confirming the adsorption of the complexes to the surface, as eluded to above. Monitoring the maximum Ln[III] emission intensity upon titration of **AuNP-[Eu.1]$^{3+}$** and **AuNP-[Tb.1]$^{3+}$** with appropriate sensitising antenna allowed determination of the number of bound complexes,[17] these studies indicated ca. 50 complexes were bound to each AuNP. Excitation of the **AuNP-[Eu.1]$^{3+}$** and **AuNP-[Tb.1]$^{3+}$** at 318 nm resulted in Stoke's-shifted fluorescence ($\lambda_{em} = 355$ nm). In the luminescence spectra (Figure 3), pseudo-Stoke's-shifted Eu[III] and Tb[III]-
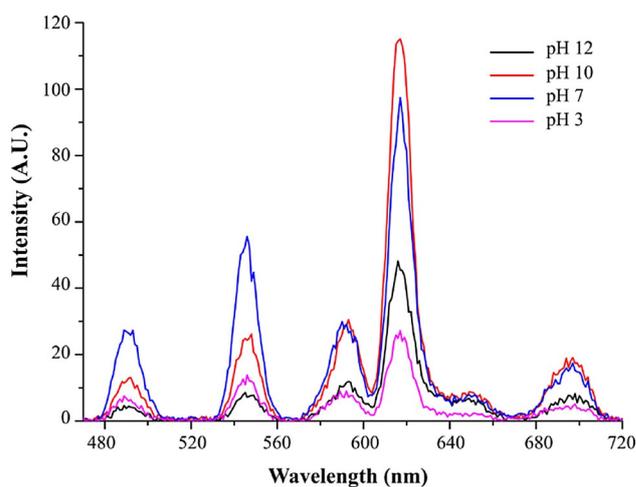

Figure 3. Overlaid time-gated emission spectra of **AuNP-[Eu.1]$^{3+}$/[Tb.1]$^{3+}$**, measured in aqueous solution at RT for pH 3, 7, 10 and 12. All measurements taken under $\lambda_{exc} = 318$ nm.

centred emissions were observed corresponding to the $^5D_0 \rightarrow {}^7F_{1-4}$ and $^5D_4 \rightarrow {}^7F_{6-3}$ transitions of the Eu[III] and Tb[III] ions, respectively. This demonstrated that the quinaldine pendent arms sensitises the Ln[III] excited states of both Eu[III] and Tb[III] when attached to the AuNP surface. Compared to **[Eu.1]$^{3+}$** and **[Tb.1]$^{3+}$** alone in aqueous solution, the emission from the AuNP-bound complexes was partially quenched. However, we and others have shown that the luminescence from emissive Ln[III] complexes can be used when attached to Au and AuNP surfaces when employing appropriate spacers and organic supports,[22] as the quenching process is distance dependent.

The responsive natures of **AuNP-[Eu.1]$^{3+}$** and **AuNP-[Tb.1]$^{3+}$** were investigated against various chemical inputs, such as pH,

pO_2 and ternary sensitising antennae (as summarised in the Supporting Information). pH spectrophotometric titrations, where both the ground and the excited states were monitored, showed that in strongly acidic media, the Eu^{III}-centred emission was quenched and subsequently enhanced with increasing pH value, reaching a maximum emission at pH 5.5. This was observed for both **[Eu.1]³⁺** and **AuNP-[Eu.1]³⁺**. The trend observed was similar to other related systems previously developed in our group.[10e, 11, 21] In contrast, the Tb^{III}-centred emission showed a subtle "off-on-off" behaviour. The Tb^{III}-centred emission was quenched in aerated strongly acidic conditions, reaching a maximum emission at pH 7, then quenching again strongly from pH 7 to 12. While the pH emission profile and emission intensity of **[Eu.1]³⁺** was independent of the presence of solvated oxygen, the **[Tb.1]³⁺** emission was enhanced in de-gassed solution, while the profile remained the same. This is due to quenching of the antenna triplet excited state through back energy transfer from the $Tb(^5D_4)$ state, as we have previously demonstrated.[21]

The logical parameterisation of the doubly functionalised **AuNP-[Eu.1]³⁺/[Tb.1]³⁺** was considered in aerated solution. The photophysical properties of mixed **AuNP-[Eu.1]³⁺/[Tb.1]³⁺** were characterised and showed similar absorption properties to the corresponding individual AuNP systems discussed above. This indicating a similar structure and surface loading of the complexes; again, titration of **AuNP-[Eu.1]³⁺/[Tb.1]³⁺** with sensitising antennae also showed ca. 50 complexes bound to each AuNP. As expected, **AuNP-[Eu.1]³⁺/[Tb.1]³⁺** gave rise to both Eu^{III}- and Tb^{III}-centred emissions and clear emission bands could be recorded. Furthermore, the relative intensities of the Eu^{III} and Tb^{III} transitions, compared to the pure **AuNP-[Eu.1]³⁺** and **AuNP-[Tb.1]³⁺** systems indicated that the AuNPs were loaded in a 1:1 ratio of **[Eu.1]³⁺** and **[Tb.1]³⁺** on the surface, as the total emission was halved in both channels. The relative intensity ratios of the Eu/Tb emissions, as well as the emission lifetimes, remained unaffected compared to that of the individual systems, showing that there was no significant $Tb(^5D_4) \rightarrow Eu(^5D_0)$ energy transfer in the initial complexes.[24] This was further supported upon the generation of the ternary complexes of **AuNP-[Eu.1]³⁺/[Tb.1]³⁺** using the nta and DMAB antennae, as the luminescence titrations (see the Supporting Information) demonstrated the existence of the desired 1:1 ratio of **[Eu.1]³⁺:[Tb.1]³⁺**, showing maximum emission intensities (following quantitative coordination of the antenna) at ca. half the intensity observed for the individual AuNPs. Despite the overlap of many emission bands, the $^5D_4 \rightarrow ^7F_{5,6}$ ($\lambda_{em} = 490, 545$ nm) and $^5D_0 \rightarrow ^7F_{1,2}$ ($\lambda_{em} = 592, 615$ nm) transitions can be considered as "pure", and suitable for monitoring the changes in the Tb^{III} and Eu^{III}, respectively.

As described above for the pure **AuNP-[Eu.1]³⁺** and **AuNP-[Tb.1]³⁺** a dependence on pH of the Ln^{III}-centred luminescence was observed for **AuNP-[Eu.1]³⁺/[Tb.1]³⁺**; the changes in Tb^{III} and Eu^{III} emission from **AuNP-[Eu.1]³⁺/[Tb.1]³⁺** with pH are shown in Figure 4. To digitise the *Input* conditions for a MLGM, the changes were considered as [H⁺] aliquots. Two separate Inputs channels, Input₁ and Input₂, could therefore be described of the same chemical species, that is, H⁺. Critical input
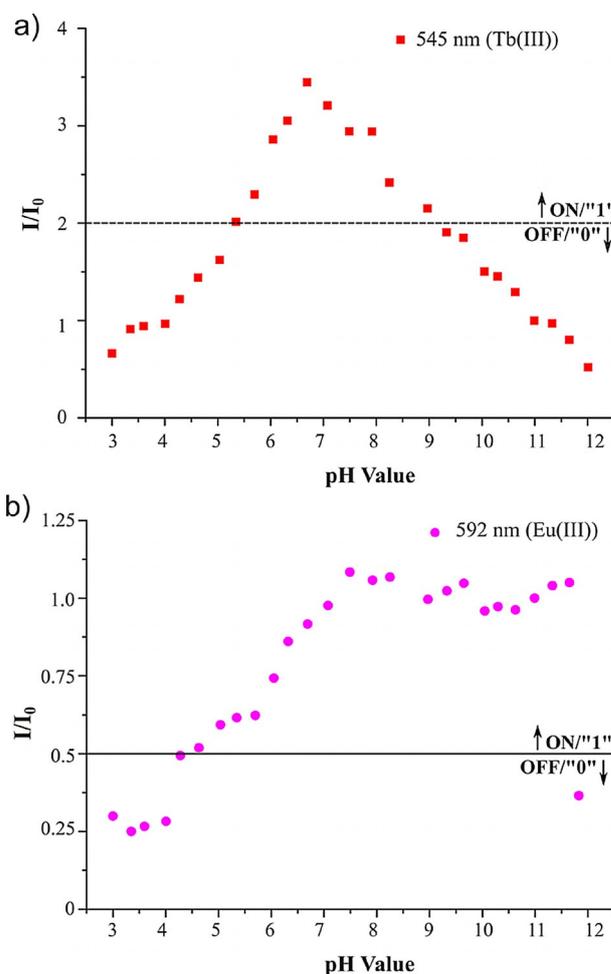

Figure 4. Changes in emission intensity with pH value and ON–OFF thresholds for: a) Tb^{III} emission at $\lambda = 545$ nm; and b) Eu^{III} at $\lambda = 592$ nm from **AuNP-[Eu.1]³⁺/[Tb.1]³⁺** in aqueous solution at RT. All measurements taken under $\lambda_{exc} = 318$ nm.

concentrations were defined such that the extreme changes were achieved rapidly. Therefore, Input₁ and Input₂ were defined as sequential increases in the order of magnitude of [H⁺] by 4 (i.e. decreasing the pH by 4 units); initial resting state set as $[H^+] = 1 \times 10^{-11}$ M. In the same manner, digitisation of the luminescence *Output*, as Output₁ and Output₂, corresponding to changes in the 545 nm and 592 nm transitions, from Tb^{III} and Eu^{III}, respectively, was achieved by placing suitable OFF/"0" to ON/"1" thresholds. These were placed such that within 10% error consistent output states were determined and selected to maximise the accessible information from the MLGM. The output thresholds, expressed in terms of I/I_0, corresponded to $I/I_0 = 2$ and 0.5 for emission at 545 nm (Tb^{III}, $^5D_4 \rightarrow ^7F_5$) and at 615 nm (Eu^{III}, $^5D_0 \rightarrow ^7F_2$), respectively, as shown in Figure 4. Applying these thresholds to the spectra yielded the truth table presented in Table 1.

The two channels corresponded to logic functions of NAND and XOR for Eu^{III} and Tb^{III} emission, respectively. In fact, this combined circuit can describe a half-subtractor device;[25] the circuit being shown in Figure 5.

Table 1. Truth table representation of $[H^+]$ parameterised MLGM from **AuNP-[Eu.1]$^{3+}$/[Tb.1]$^{3+}$** and the corresponding mimicked logic functions.

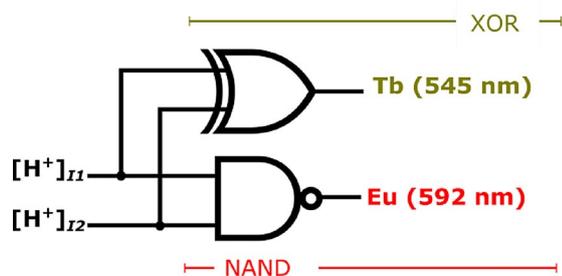| Input$_1$ [H$^+$]	Input$_2$ [H$^+$]	Output$_1$ $\lambda_{em} = 545$ nm	Output$_2$ $\lambda_{em} = 592$ nm
0	0	0	1
1	0	1	1
0	1	1	1
1	1	0	0

Figure 5. Logic circuit describing the behaviour of **AuNP-[Eu.1]$^{3+}$/[Tb.1]$^{3+}$** with $[H^+]$ inputs.

The formation of ternary complexes was also considered. DMAB and nta coordinate through carboxylate and β-ketonate moieties, respectively, and the corresponding ternary complex with nta exhibiting greater stability due to the less strained geometry. The relative stabilities of these allowed for selective displacement of DMAB by nta without a strong reverse equilibrium, giving the characteristic states for each combination of Inputs required for robust logical analysis. Furthermore, the relative sensitisation efficiencies gave "selective" Eu^{III} and Tb^{III} emission by nta and DMAB, respectively, under aerobic conditions. Once more, critical input concentrations were defined such that the extreme changes were achieved rapidly. The maximum response was recorded at ≈50 equivalents (4×10^{-6} M) of nta or DMAB vs. the AuNP concentration (1×10^{-7} M). This corresponded to the quantitative coordination of the bound complexes. However, the system was operated at extreme Input conditions (i.e. stoichiometric excesses). For Input$_1$ and Input$_2$ these were defined to be ON/"1" only when [nta] or [DMAB] = 120[AuNP], respectively. The emission spectra in the ternary complexes showed a different band ratiometry and relative intensities (this is the results of more efficient population of the Eu($^5D_0$) than Tb($^5D_4$) states by the ternary antennae). Since the emission from Tb^{III} was partially quenched (by ca. 5% in excess DMAB after the maximum emission), the Tb^{III} output threshold was assigned as $I/I_0 = 4.5$, Figure 6c. For Eu^{III} emission, the output threshold of $I/I_0 = 180$ was applied following the same criteria described above, Figure 6d. The luminescence spectra were recorded under the four combinations of Input$_1$ (nta) and Input$_2$ (DMAB), as shown and summarised in Figure 6. In each case, using the proposed thresholds, the normalised intensities were parameterised against the (0,0) initial resting state. These corresponding truth table is shown in Table 2.
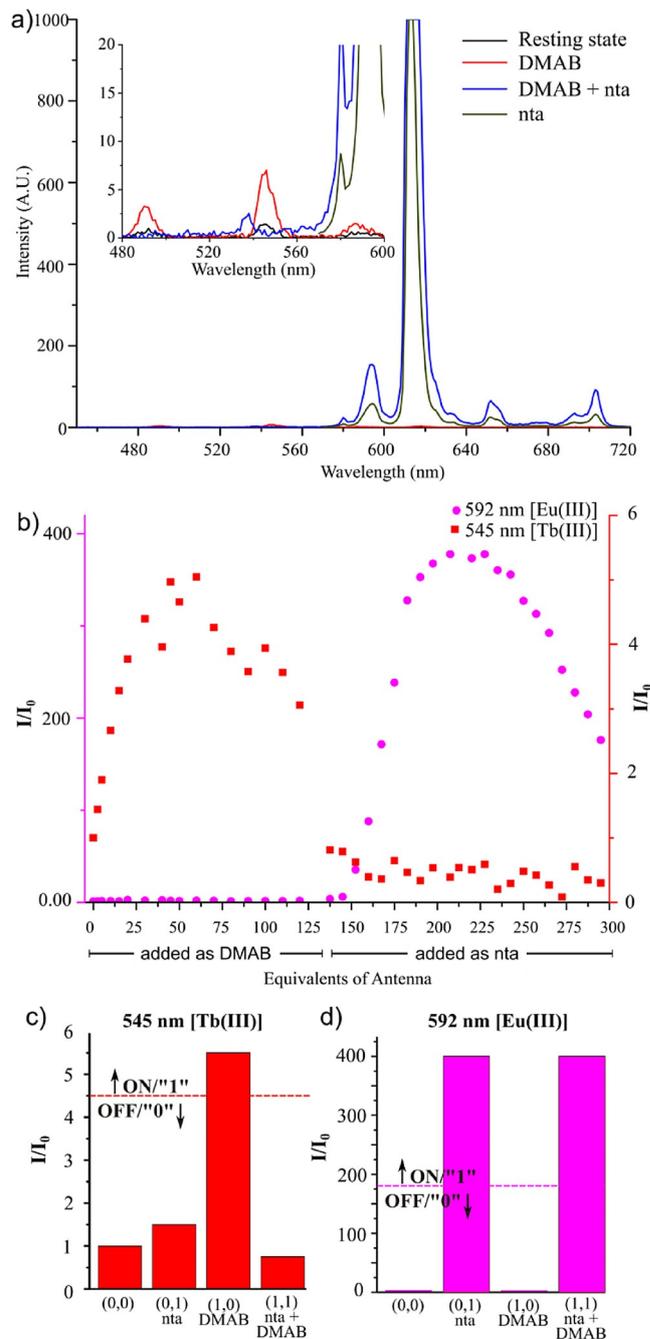

Figure 6. a) Overlaid time-gated emission spectra of **AuNP-[Eu.1]$^{3+}$/[Tb.1]$^{3+}$** upon titration of DMAB and nta; b) relative emission intensities measured at $\lambda = 545$ and 592 nm from Tb^{III} and Eu^{III}, respectively, during titration with DMAB and nta; and c) relative emission changes when treated with various combinations of DMAB and nta corresponding to logical input states. All measurements taken under $\lambda_{exc} = 318$ nm.

In the (0,0) state, both Eu^{III} and Tb^{III} output channels were OFF/"0". The addition of nta generated the (1,0) state; the Eu^{III} emission became ON/"1" while Tb^{III} emission remained OFF/"0", consistent with the sensitisation efficiency of the nta antenna. In contrast, the addition of DMAB alone gave the (0,1) state; resulting in the change of Tb^{III} emission to ON/"1", while Eu^{III} emission remained OFF/"0". The final Input state (1,1) was obtained from the addition of both DMAB and nta, resulting in

Table 2. Truth table representation of [nta], [DMAB] parameterised MLGM from AuNP-[Eu.1]$^{3+}$/[Tb.1]$^{3+}$ and the corresponding mimicked logic functions.

Input$_1$ [DMAB]	Input$_2$ [nta]	Output$_1$ $\lambda_{em} = 545$ nm	Output$_2$ $\lambda_{em} = 592$ nm
0	0	0	0
1	0	1	0
0	1	0	1
1	1	0	1

ing)[27] can lead to information- and logic-rich targeted sensor devices. Research of this nature continues within our laboratory.

Acknowledgements

Eu^{III} emission as ON/"1" and Tb^{III} emission as OFF/"0". The switching behaviour, and consistent output condition, in the (1,1) state agreed with the relative stabilities of the ternary complexes of nta and DMAB. As this is an equilibrium process, the same output state was achieved from sequential addition of nta then DMAB, DMAB then nta, or simultaneous addition of both. While the displacement of DMAB and preferential binding of nta is key to the change in output channels between the (1,0) and the (1,1) input states, a limitation of the MLGM can be identified. This mechanism of action resulted in an inability to switch the device back to a previous state. Therefore, this MLGM represents a mechanism suitable only for single-use devices and a logic function with permanent memory of the output. However, these are common in POC diagnostics and small medical devices.[26] The Eu^{III} and Tb^{III} output channels, shown in Table 2, corresponded simple logic mimics.

Since the Eu^{III} emission was only ON/"1" in the presence of nta, the output corresponded a YES function within a two-input system and can be characterised as TRANSFER$_{[nta]}$. The Tb^{III} output reported ON/"1" only in the case where DMAB was present alone, corresponding to INHIBIT$_{[nta]}$ (see Figure 7).
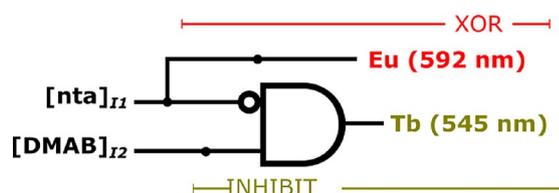
Conflict of interest

The authors declare no conflict of interest.

Figure 7. Logic circuit describing the behaviour of **AuNP-[Eu.1]$^{3+}$/[Tb.1]$^{3+}$** with [DMAB] and [nta] inputs.

In summary, we have demonstrated the immobilisation of multi-stimuli responsive luminescent cyclen complexes on the surface of AuNPs, and the analysis of their response in terms of logic functions. Mixed Eu^{III}:Tb^{III} AuNPs were sensitive to both pH and antennae identities which allowed the construction of two logic circuits of XOR-NAND (half-subtractor) with [H$^+$] inputs and TRANSFER-INHIBIT with [nta] and [DMAB] inputs. The XOR-NAND circuit is reversible and reusable, while the TRANSFER-INHIBIT circuit could not return from the (1,1) state. This system reported herein was also sensitive to pO$_2$, however this was not exploited on this occasion. However, we highlight that such Ln^{III} systems have rich sensitivity and the application of logic analysis to mixed sensor arrays (as in ratiometric sens-

[1] a) D. E. Barry, D. F. Caffrey, T. Gunnlaugsson, *Chem. Soc. Rev.* **2016**, *45*, 3244 – 3274; b) H. Xu, C.-S. Cao, X.-M. Kang, B. Zhao, *Dalton Trans.* **2016**, *45*, 18003 – 18017; c) H. Ihara, M. Takafuji, Y. Kuwahara, *Polym. J.* **2016**, *48*, 843 – 853; d) Y. Sagara, S. Yamae, M. Mitani, C. Weder, T. Kato, *Adv. Mater.* **2016**, *28*, 1073 – 1095; e) L. Maggini, D. Bonifazi, *Chem. Soc. Rev.* **2012**, *41*, 211 – 241.

[2] a) A. Aviram, *J. Am. Chem. Soc.* **1988**, *110*, 5687 – 5692; b) A. P. de Silva, N. H. Gunaratne, C. P. McCoy, *Nature* **1993**, *364*, 42 – 44; c) A. P. de Silva, I. M. Dixon, H. Q. N. Guarantna, T. Gunnlaugsson, P. R. S. Maxwell, T. E. Rice, *J. Am. Chem. Soc.* **1999**, *121*, 1393 – 1394; d) A. P. de Silva, S. Uchiyama, *Nat. Nanotechnol.* **2007**, *2*, 399 – 410.

[3] a) M. Strianese, C. Pellecchia, *Coord. Chem. Rev.* **2016**, *318*, 16 – 28; b) Z. Liu, W. He, Z. Guo, *Chem. Soc. Rev.* **2013**, *42*, 1568 – 1600; c) S. Pope, T. Gunnlaugsson in *Luminescence of Lanthanide Ions in Coordination Compounds and Nanomaterials* (Ed.: A. de Bettencourt-Dias), Wiley, Hoboken, **2014**, pp. 231 – 267; d) X. Wang, H. Chang, J. Xie, B. Zhao, B. Liu, S. Xu, W. Pei, N. Ren, L. Huang, W. Huang, *Coord. Chem. Rev.* **2014**, *273 – 274*, 201 – 212.

[4] a) K. Singh, D. Sareen, P. Kaur, H. Miyake, H. Tsukube, *Chem. Eur. J.* **2013**, *19*, 6914 – 6936; b) K.-C. Chang, S. S. Sun, M. O. Odago, A. J. Lees, *Coord. Chem. Rev.* **2015**, *284*, 111 – 123; c) R. M. Duke, J. E. O'Brien, T. McCabe, T. Gunnlaugsson, *Org. Biomol. Chem.* **2008**, *6*, 4089 – 4092; d) T. Gunnlaugsson, B. Bichell, C. Nolan, *Tetrahedron Lett.* **2002**, *43*, 4989 – 4992.

[5] a) A. P. de Silva, S. Uchiyama, T. P. Vance, B. Wannalerse, *Coord. Chem. Rev.* **2007**, *251*, 1623 – 1632; b) A. P. de Silva, *Beilstein J. Org. Chem.* **2015**, *11*, 2774 – 2784.

[6] J. Andréasson, U. Pischel, *Chem. Soc. Rev.* **2015**, *44*, 1053 – 1069.

[7] U. Pischel, *Chimia* **2014**, *68*, 505 – 511.

[8] A. P. de Silva, *Molecular Logic-Based Computation*, RSC Publishing, London, **2013**, pp. 1 – 11.

[9] a) E. B. Veale, J. A. Kitchen, T. Gunnlaugsson, *Supramol. Chem.* **2013**, *25*, 101 – 108.

[10] a) E. M. Surender, S. J. Bradberry, S. A. Bright, C. P. McCoy, D. C. Williams, T. Gunnlaugsson, *J. Am. Chem. Soc.* **2017**, *139*, 381 – 388; b) S. J. Bradberry, A. J. Savyasachi, M. Martinez-Calvo, T. Gunnlaugsson, *Coord. Chem. Rev.* **2014**, *273 – 274*, 226 – 241; c) H. M. Burke, T. Gunnlaugsson, E. M. Scanlan, *Org. Biomol. Chem.* **2016**, *14*, 9133 – 9145; d) C. M. G. dos Santos, P. B. Fernández, S. E. Plush, J. P. Leonard, T. Gunnlaugsson, *Chem. Commun.* **2007**, 3389 – 3391; e) T. Gunnlaugsson, D. Parker, *Chem. Commun.* **1998**, 511 – 512.

[11] C. S. Bonnet, T. Gunnlaugsson, *New J. Chem.* **2009**, *33*, 1025–1030.

[12] a) S. V. Eliseeva, J.-C. G. Bünzli in *Lanthanide Luminescence* (Ed.: M. Hof), Springer, Berlin, **2011**, pp. 1–45; b) C. M. G. dos Santos, A. J. Harte, S. J. Quinn, T. Gunnlaugsson, *Coord. Chem. Rev.* **2008**, *252*, 2512–2527; c) J. Leonard, C. Nolan, F. Stomeo, T. Gunnlaugsson, *Top. Curr. Chem.* **2007**, *281*, 1–43; d) J.-C. G. Bünzli, *Chem. Rev.* **2010**, *110*, 2729–2755; e) S. Faulkner, L. S. Natrajan, W. S. Perry, D. Sykes, *Dalton Trans.* **2009**, 3890–3899; f) M. D. Ward, *Coord. Chem. Rev.* **2007**, *251*, 1663–1677; g) W. S. Perry, S. J. A. Pope, C. Allain, B. J. Coe, A. M. Kenwright, S. Faulkner, *Dalton Trans.* **2010**, *39*, 10974–10983.

[13] A. P. de Silva, *Molecular Logic-Based Computation*, RSC Publishing, London, **2013**, pp. 24–33.

[14] S. J. Bradberry, J. P. Byrne, C. P. McCoy, T. Gunnlaugsson, *Chem. Commun.* **2015**, *51*, 16565–16568.

[15] a) J. C. Claussen, W. R. Algar, N. Hildebrandt, K. Susmu, M. G. Ancona, I. L. Medintz, *Nanoscale* **2013**, *5*, 12156–12170; b) J. C. Claussen, N. Hildebrandt, K. Susmu, M. G. Ancona, I. L. Medintz, *ACS Appl. Mater. Interfaces* **2014**, *6*, 3771–3778.

[16] a) B. Liu, J. Liu, *Anal. Methods* **2017**, *9*, 2633–2643; b) Z. Wang, L. Ma, *Coord. Chem. Rev.* **2009**, *253*, 1607–1618; c) R. A. Sperling, P. Rivera Gil, F. Zhang, M. Zanella, W. J. Parak, *Chem. Soc. Rev.* **2008**, *37*, 1896–1908; d) S. Comby, E. M. Surender, O. Kotova, L. K. Truman, J. K. Molloy, T. Gunnlaugsson, *Inorg. Chem.* **2014**, *53*, 1867–1879.

[17] E. M. Surender, S. Comby, B. L. Cavanagh, O. Brennan, T. C. Lee, T. Gunnlaugsson, *Chem* **2016**, *1*, 438–455.

[18] E. M. Surender, S. Comby, S. Martyn, B. Cavanagh, T. C. Lee, D. F. Brougham, T. Gunnlaugsson, *Chem. Commun.* **2016**, *52*, 10858–10861.

[19] a) S. Comby, T. Gunnlaugsson, *ACS Nano* **2011**, *5*, 7184–7197; b) J. P. Leonard, C. M. G. dos Santos, S. E. Plush, T. McCabe, T. Gunnlaugsson, *Chem. Commun.* **2007**, 129–131.

[20] a) O. Kotova, S. Comby, T. Gunnlaugsson, *Chem. Commun.* **2011**, *47*, 6810–6812; b) D. F. Caffrey, T. Gunnlaugsson, *Dalton Trans.* **2014**, *43*, 17964–17970.

[21] a) T. Gunnlaugsson, D. A. MacDonaill, D. Parker, *J. Am. Chem. Soc.* **2001**, *123*, 12866–12876; b) T. Gunnlaugsson, D. A. MacDonaill, D. Parker, *Chem. Commun.* **2000**, 93–94.

[22] a) L. K. Truman, S. Comby, T. Gunnlaugsson, *Angew. Chem. Int. Ed.* **2012**, *51*, 9624–9627; *Angew. Chem.* **2012**, *124*, 9762–9765; b) C. S. Bonnet, J. Massue, S. J. Quinn, T. Gunnlaugsson, *Org. Biomol. Chem.* **2009**, *7*, 3074–3078; c) A. C. Savage, Z. Pikramenou, *Chem. Commun.* **2011**, *47*, 6431–6433; d) A. Davies, D. J. Lewis, S. P. Watson, S. G. Thomas, Z. Pikramenou, *Proc. Natl. Acad. Sci. USA* **2012**, *109*, 1862–1867.

[23] a) J. Massue, S. J. Quinn, T. Gunnlaugsson, *J. Am. Chem. Soc.* **2008**, *130*, 6900–6901; b) M. Brust, M. Walker, D. Bethell, D. J. Schiffrin, R. Whyman, *J. Chem. Soc. Chem. Commun.* **1994**, 801–802.

[24] Q. Li, T. Li, J. Wu, *J. Phys. Chem. B* **2001**, *105*, 12293–12296.

[25] U. Pischel, B. Heller, *New J. Chem.* **2008**, *32*, 395–400.

[26] a) H. N. Chan, Y. Shu, B. Xiong, Y. Chen, Y. Chen, Q. Tian, S. A. Michael, B. Shen, H. Wu, *ACS Sens.* **2016**, *1*, 227–234; b) A. Hierlemann, R. Gutierrez-Osuna, *Chem. Rev.* **2008**, *108*, 563–613; c) B. C. Janegitz, J. Cancino, V. Zucolotto, *J. Nanosci. Nanotechnol.* **2014**, *14*, 378–389.

[27] a) D. Kovacs, X. Lu, L. S. Mészáros, M. Ott, J. Andres, K. E. Borbas, *J. Am. Chem. Soc.* **2017**, *139*, 5756–5767; b) G.-L. Law, R. Pal, L. O. Palsson, D. Parker, K.-L. Wong, *Chem. Commun.* **2009**, 7321–7323; c) S. E. Plush, T. Gunnlaugsson, *Dalton Trans.* **2008**, 3801–3804; d) D. Parker, R. Pal, *Org. Biomol. Chem.* **2008**, *6*, 1020–1033; e) D. Parker, R. Pal, *Chem. Commun.* **2007**, 474–476.